ELSEVIER

Journal of Alloys and Compounds 356–357 (2003) 673–678

Journal of ALLOYS AND COMPOUNDS

www.elsevier.com/locate/jallcom

Hydrogenation induced valence change and metal atom site exchange at room temperature in the C14-type sub-structure of $CeMn_{1.8}Al_{0.2}H_{4.4}$

Y.E. Filinchuk[a], D. Sheptyakov[b], G. Hilscher[c], K. Yvon[a,*]

[a]*Laboratoire de Cristallographie, University of Geneva, 24 Quai Ernest-Ansermet, CH-1211 Geneva 4, Switzerland*
[b]*Laboratory for Neutron Scattering, ETHZ & PSI, CH-5232 Villigen PSI, Switzerland*
[c]*Institut für Experimentalphysik, Technical University, Vienna, Austria*

Received 27 August 2002; received in revised form 1 October 2002; accepted 7 December 2002

Abstract

$CeMn_{1.8}Al_{0.2}$ absorbs more than 4.4 hydrogen atoms near ambient conditions, thereby undergoing a volume expansion ($\Delta V/V$~43%) that is the largest known among metal hydrides. While the Mn/Al distribution in the C14-type alloy [$P6_3/mmc$, $a=5.37393(6)$, $c=8.76321(12)$ Å] is partially ordered (preference of Al for site 2*a*), it tends to become disordered in the hydride (equal Mn/Al occupancies for sites 2*a* and 6*h*). Only very slow hydrogenation while cooling the sample to -70 °C is capable of maintaining a partial Mn/Al order. Deuterium in $CeMn_{1.8}Al_{0.2}D_{4.36(7)}$ [$a=5.9788(6)$, $c=9.7600(13)$ Å] occupies exclusively tetrahedral $Ce_2(Mn,Al)_2$ type interstices. Magnetic susceptibility data suggest that the volume expansion during hydrogenation is enhanced by a valence change of cerium ($Ce^{IV}\rightarrow Ce^{III}$).

Keywords: Hydrogen storage materials; Magnetic measurements; Valence change; Crystal structure; Neutron diffraction

1. Introduction

The solid solution series $Ce(Mn_{1-x}Al_x)_2$ crystallises with a hexagonal C14-type structure in the range $0.15<x<0.35$ and a cubic C15-type structure for $x>0.35$ and $x<0.1$ [1]. Binary $CeMn_2$ ($x=0$) does not seem to exist. A recent in-situ neutron diffraction study of hexagonal $CeMn_{1.5}Al_{0.5}$ ($x=0.25$) as a function of deuterium pressure has shown [2] that the compound absorbs up to ~four deuterium atoms per formula unit (f.u.) at room temperature and 25 bar pressure, thereby undergoing a lattice expansion of ~34%. The authors concluded that the Mn and Al atoms on the two available sites in the structure (2*a* and 6*h* in the space group $P6_3/mmc$) were distributed at random in both the alloy and the deuteride. In this paper we report on the synthesis, structure and hydrogenation properties of a more Mn rich alloy of composition $CeMn_{1.8}Al_{0.2}$ ($x=0.1$). It will be shown that this compound absorbs ~10% more hydrogen (~4.4 H/f.u.) than the previously investigated one, and undergoes a volume expansion of ~43% that is the biggest known among reversible metal hydrides. Diffraction data reveal a partially ordered Mn/Al atom distribution that tends to become disordered during hydrogenation. Magnetic measurements show a hydrogenation induced valence change of cerium ($Ce^{IV}\rightarrow Ce^{III}$).

2. Experimental

2.1. Synthesis of alloys

Samples of nominal composition $CeMn_{1.8}Al_{0.2}$ were prepared by arc-melting mixtures of high purity elements (Ce: Ames Lab., ingot, 99.93%; Mn: Kochlight, pieces, 99.99%; Al: JMC, wire, 99.999%) at a small excess of cerium (3 wt.%). The ingots (~3 g) were sealed into quartz tubes under 0.3 bar argon pressure and annealed at 700 °C for up to 8 weeks. They were essentially single phase and crystallised with a hexagonal C14-type structure. Those annealed for a week (samples **1**–**3**) contained traces of α-Mn while those annealed for 2 months (samples **4** and **5**) contained some β-Mn.

*Corresponding author. Tel.: +41-22-702-6231; fax: +41-22-702-6864.
E-mail address: klaus.yvon@cryst.unige.ch (K. Yvon).

0925-8388/03/$ – see front matter
doi:10.1016/S0925-8388(03)00123-3

2.2. Hydogenation (deuteration)

The alloys **3**–**5** were hydrogenated (deuterated) under a pressure of 0.2–3 bar in a stainless autoclave (D_2 purity 99.4%). Considerable difficulties were encountered to obtain reproducible results because the hydrogenation properties depended not only on obvious parameters such as temperature, pressure and time, but also on less obvious parameters such as hydrogenation speed, grain size and total sample mass. Generally, rapid hydrogenation at room temperature of coarse powders having a large mass lead to substantial diffraction peak broadening and/or disproportionation of the alloy into binary Ce hydride and manganese. To reduce these undesirable effects, hydrogenation was carried out at low temperature on finely ground and sieved powders of small mass. The best results (i.e. large hydrogen contents, little disproportionation, good sample crystallinity) were obtained on powders not exceeding 25 μm in grain size and 3 g in total mass that were hydrogenated (deuterated) at −70 °C by using a cooling mixture of solid carbon dioxide and acetone. For sample **3**, the hydrogen pressure was increased stepwise during 4 h up to 3 bar and left at that level for 15 h. For samples **4** and **5**, deuterium/argon mixtures were used, the pressure of which was increased stepwise during 8 h to 2 bar and left at that level for 15 h. In order to reduce lattice strain and favour a possible Mn/Al rearrangement in the structure, sample **5** was annealed at 175 °C and 2 bar D_2 pressure. Annealing above 200 °C lead to sample disproportionation. All samples were highly pyrophoric and had to be handled carefully. They were relatively unstable and lost hydrogen (deuterium) under ambient conditions (argon). While hydride **3** was measured rapidly and found to contain a large (but not quantified) amount of hydrogen, the deuterides **4** and **5** were measured later and found to contain a smaller amount of deuterium that was quantified by diffraction experiments (see below).

2.3. Diffraction studies and structure refinements

The samples were investigated by X-ray and neutron diffraction and their structures refined by using the known structure model of the hexagonal C14-type Laves phase AB_2 and its deuteride AB_2D_x [A = Ce on site 4*f*, B = Mn/Al on sites 2*a* (B1) and 6*h* (B2) of space group $P6_3/mmc$; D in four tetrahedral (A_2B_2) type interstices]. For sample **1** single crystals were isolated from the surface of the annealed ingot and investigated on a Stoe IPDS image plate diffractometer (Mo Kα radiation). During structure refinement the total occupancy (Al + Mn) of each metal site (B1, B2) was constrained to 100% but left unconstrained with respect to the Mn/Al ratio, and individual anisotropic displacement parameters were used. Samples **2**–**5** were investigated by powder X-ray (**2**, **3**: Bruker D8 Advance diffractometer, Cu $K\alpha_1$ radiation) and neutron diffraction (**4**, **5**: HRPT [3] at SINQ, PSI, Villigen, $\lambda = 1.494$ Å). All samples contained a C14-type majority phase. While the alloy **2** was practically single-phase, the hydride **3** and the deuterides **4** and **5** contained considerable amounts of secondary phases due to disproportionation (mainly manganese metal and cerium based impurities). During structure refinement the occupancies of the metal sites of the C14-type phase were constrained with respect to both their sums (Mn + Al = 100% for B1 and B2 each) and nominal composition (Mn/Al = 9). Isotropic displacement parameters were used and constrained to be equal. Refined cell parameters and occupancy factors of the metal sites for the various samples are summarized in Table 1. Detailed structure results are given only for the deuterides **4** and **5** as shown in Table 2. Structure data for the other samples will be presented elsewhere. The neutron patterns of sample **4** are shown in Fig. 1 and a partial view of the $CeMn_{1.8}Al_{0.2}D_{\sim 4.4}$ structure is given in Fig. 2.

2.4. Magnetic susceptibility

Magnetic measurements on the alloy **2**, the hydride **3** and the deuterides **4** and **5** were performed by using a SQUID magnetometer. The comparison of the d.c. susceptibilities (M/H) of $CeMn_{1.8}Al_{0.2}$ and $CeMn_{1.8}Al_{0.2}D_{3.5}$ in Fig. 3 demonstrates the significant influence of deuterium (hydrogen) uptake on the magnetic properties in these compounds.

3. Results and discussion

3.1. Hydrogenation induced volume increase

The volume increase during hydrogenation (deuteration) of the presently studied compounds (**3** $CeMn_{1.8}Al_{0.2}H_x$: $\Delta V/V = 42.5\%$; **4** $CeMn_{1.8}Al_{0.2}D_{\sim 4.4}$: $\Delta V/V = 37.9\%$) is

Table 1
Cell parameters and refined aluminium occupancies of B1 and B2 sites of the C14 type structure of $CeMn_{1.8}Al_{0.2}$ alloys and their hydrides (deuterides)

Sample	Cell parameters	Method	Al(B1)	Al(B2)
1 Alloy $CeMn_{1.8}Al_{0.2}$	$a = 5.3980(10)$, $c = 8.806(2)$ Å, $V = 222.21(8)$ Å^3	Single crystal X-ray	0.18(2)	0.10(1)
2 Alloy $CeMn_{1.8}Al_{0.2}$	$a = 5.37393(6)$, $c = 8.76321(12)$ Å, $V = 219.169(5)$ Å^3	Powder X-ray	0.284(9)	0.039(3)
3 Hydride $CeMn_{1.8}Al_{0.2}H_x$	$a = 6.0559(6)$, $c = 9.8442(11)$ Å, $V = 312.66(6)$ Å^3	Powder X-ray	0.12(2)	0.093(7)
4 Deuteride $CeMn_{1.8}Al_{0.2}D_{4.37}$	$a = 5.9788(6)$, $c = 9.7600(13)$ Å, $V = 302.14(6)$ Å^3	Powder neutrons	0.296(12)	0.035(4)
5 Annealed deuteride $CeMn_{1.8}Al_{0.2}D_{3.52}$	$a = 5.9353(8)$, $c = 9.7641(17)$ Å, $V = 297.88(8)$ Å^3	Powder neutrons	0.033(12)	0.123(4)

E.S.D.s in parentheses.

Table 2
Neutron powder diffraction refinement results on deuteride samples **4** (first lines) and **5** (second lines, in italics)

Atom (site)	*x*	*y*	*z*	B_{iso}	Occupancy
Ce (4*f*)	1/3	2/3	0.0644(5)	0.40(5)	1.0(–)
			0.0639(6)	*1.19(8)*	1.0(–)
Mn1 (2*a*)	0	0	0	1.53(8)	0.704(12)
				2.25(9)	*0.967(12)*
Al1 (2*a*)					0.296(12)
					0.033(12)
Mn2 (6*h*)	0.8390(11)	2*x*	1/4	1.53(8)	0.965(4)
	0.8386(17)			*2.25(9)*	*0.877(4)*
Al2 (6*h*)					0.035(4)
					0.123(4)
D1 (24*l*)	0.0581(7)	0.3120(9)	0.5731(6)	2.26(6)	0.312(4)
	0.0571(7)	*0.3030(8)*	*0.5728(5)*	*1.42(6)*	*0.260(4)*
D2 ($12k_2$)	0.4536(11)	2*x*	0.6424(6)	2.26(6)	0.407(7)
	0.4512(15)		*0.6408(9)*	*1.42(6)*	*0.237(6)*
D3 ($6h_2$)	0.487(3)	2*x*	1/4	2.26(6)	0.267(7)
	0.496(2)			*1.42(6)*	*0.274(7)*
D4 ($6h_1$)	0.1882(12)	2*x*	1/4	2.26(6)	0.580(8)
	0.1798(17)			*1.42(6)*	*0.412(7)*

E.S.D.s in parentheses.
4: Refined composition $CeMn_{1.8}Al_{0.2}D_{4.36(7)}$, agreement indices: $R_B = 4.16\%$, $R_p = 15.7\%$, $R_{wp} = 15.8\%$, $S = 3.10$; secondary phases CeD_x (5.6%) and β-Mn (21.3%).
5: Refined composition $CeMn_{1.8}Al_{0.2}D_{3.52(6)}$, agreement indices: $R_B = 4.59\%$, $R_p = 16.8\%$, $R_{wp} = 15.0\%$, $S = 2.68$; secondary phases CeD_x (8.6%) and β-Mn (18.2%).

much bigger than that of previously investigated more Al rich compositions ($CeMn_{1.5}Al_{0.5}D_{\sim 3.6}$ obtained at 2.7 bar H_2 pressure: $\Delta V/V = 30.1\%$ [2]). It is the largest known so far for reversible metal hydrides. Given the usually observed volume increments in Laves phase hydrides (~2.5–3 $Å^3$/D atom), those in the present compounds (**4**: ~4.75 $Å^3$/D atom) cannot be exclusively due to the space requirement of hydrogen and suggest the onset of a valence transition of cerium ($Ce^{IV} \rightarrow Ce^{III}$). Large hydrogen induced volume expansions are not uncommon in cerium based intermetallics as shown by $CeCo_3H_4$ for which the rhombohedral *c* axis increases by more than 30% [4], and $CeRu_2H_5$ for which the cell volume increases by ~37% [5]. For the latter, neutron diffraction experiments [6] and X-ray photoemission spectroscopy data [7] have provided evidence for hydrogen induced magnetic ordering. A hydrogen induced valence transition was also found in the nickel analogue $CeNiAlH_x$ as shown by

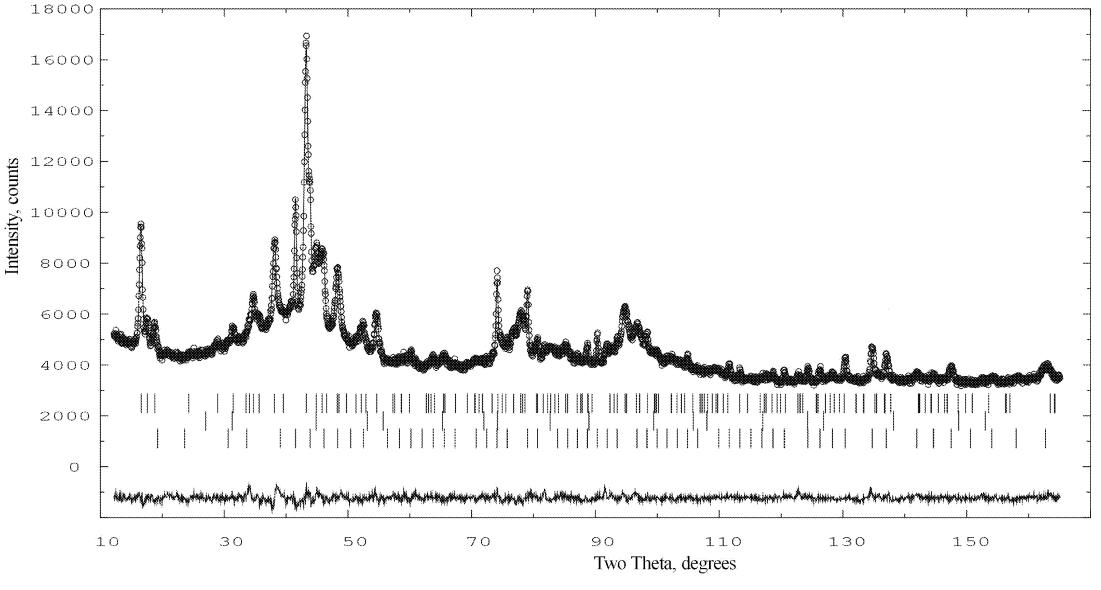

Fig. 1. Observed (circles) calculated (line) and difference (bottom) neutron powder diffraction patterns of the deuteride $CeMn_{1.8}Al_{0.2}D_{4.36(7)}$ (sample **4**, $\lambda = 1.494$ Å). Vertical bars indicate Bragg positions of main phase, CeD_3 and Mn (from top to bottom). Broad maxima correspond to diffraction orders $n = 1, 2$ for short-range ordered D–D distances of 2.1 Å.

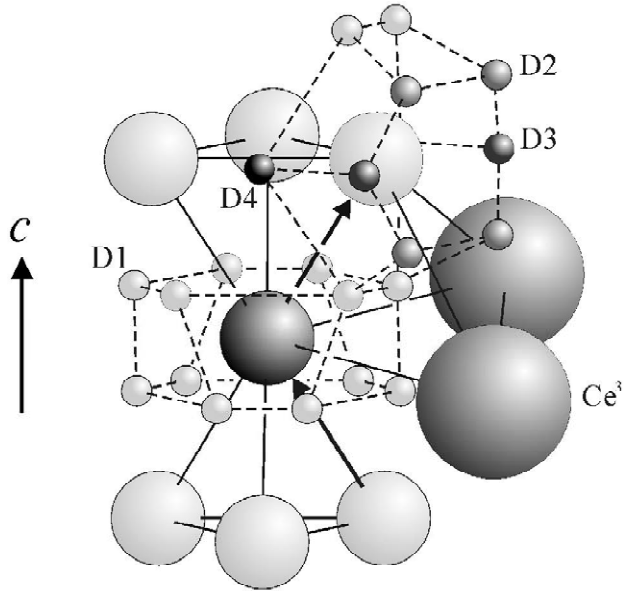

Fig. 2. Partial view of the hexagonal Laves phase derivative structure of $CeMn_{1.8}Al_{0.2}D_{4.4}$. Large spheres Ce, medium spheres Mn(Al), small spheres deuterium (sites numbered). During hydrogenation aluminum atoms migrate from B1 (dark spheres) to B2 (light spheres), and manganese from B2 to B1 (see arrows).

magnetic measurements [8] but not in the cubic representatives of the present series such as $CeMnAlH_{2.4}$ for which the volume expansion is <7% [9]. This behaviour is consistent with earlier suggestions [10] concerning the valence state of cerium in $Ce(Mn_{1-x}Al_x)_2$ alloys that is Ce^{III}-like in Al rich (cubic) and Ce^{IV}-like in Al poor (hexagonal) compositions.

3.2. Metal atom site preference

The two B metal sites in the structure are not occupied at random, at least not in the alloys **1** and **2** for which aluminium clearly prefers B1 over B2 (see Table 1). A deviation from random occupancy of these sites is not surprising because they are crystallographic non-equivalent. While B1 (site 2*a*, $\bar{3}m$ symmetry) joins double-tetrahedrons of B-atoms *via* corners to chains running along the hexagonal axis, B2 (site 6*h*, *mm*2 symmetry) forms the triangular base of the double-tetrahedrons (see Fig. 2). Surprisingly, however, this site preference is attenuated in the hydrides (deuterides). In **3**, for example, the B sites show nearly random occupancy [12(2)% Al for B1 and 9(1)% Al for B2, compared to 10% Al for random occupancy]. In other words, a significant fraction of aluminium (**3**: ~40%) has migrated during hydrogenation from B1 to B2 (and manganese from B2 to B1) thus increasing the structural disorder. This is the first time that such a hydrogenation induced rearrangement of metal atom is detected in Laves phase compounds. Interestingly, the refined Al occupancies of the (non-annealed) deuteride **4** that has been prepared at a slower speed of deuteration than hydride **3** shows no increase of disorder [30(1)% Al for B1, 3.5(4)% Al for B2]. This suggests that slow hydrogenation of the alloy helps to maintain partial order in the B atom substructure. On the other hand, the annealed deuteride **5** shows the opposite trend, i.e. aluminium prefers site B2 [0.123(4)] rather than B1 [0.033(12)]. Altogether, the findings suggest that the observed hydrogen-induced rearrangement in the Mn/Al atom substructure is the consequence of a strongly exothermic hydrogenation reaction. Although the temperature

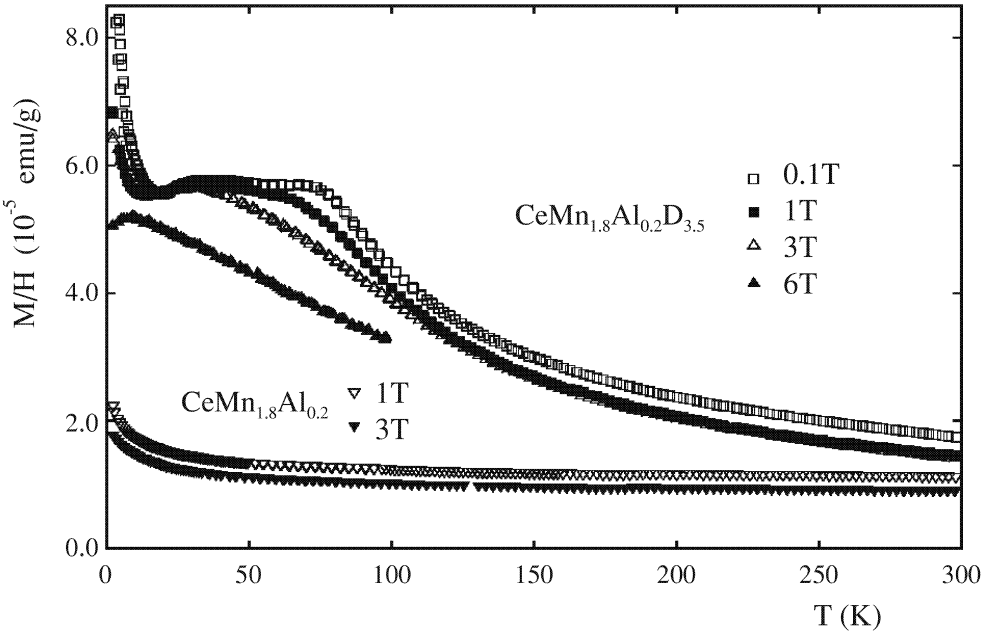

Fig. 3. Susceptibility (M/H) after zero-field cooling as a function of temperature for $CeMn_{1.8}Al_{0.2}$ and $CeMn_{1.8}Al_{0.2}D_{3.5}$.

of the sample environment during the reaction was kept rather low (−70 °C) it did presumably not prevent individual metal grains from heating up and inducing an atom exchange between nearest neighbour sites (see B1 and B2 in Fig. 2). Such a picture is consistent with the observed dependence of hydrogenation on experimental conditions such as speed of hydrogenation, grain size and sample mass.

3.3. Influence of aluminum content on hydrogenation properties

Similar to the cubic series $Ce(Mn_{1-x}Al_x)_2$ ($0.5<x<1$) [11] the relatively Al rich composition $CeMn_{1.5}Al_{0.5}$ [2] of the hexagonal series absorbs less hydrogen than the Al poorer composition $CeMn_{1.8}Al_{0.2}$. For the cubic series the decrease of hydrogen capacity as a function of Al content has been modeled by a statistical analysis [11] and attributed to a preferential hydrogen occupancy of Al free metal tetrahedra [Ce_2Mn_2] at the expense of Al containing tetrahedra [Ce_2AlMn] and [Ce_2Al_2]. A similar model also appears to be applicable for the present hexagonal series because the average number of metal–deuterium contacts per B atom site, N_D, in **4** $CeMn_{1.8}Al_{0.2}D_{\sim 4.4}$ is smaller for the more Al rich site B1 ($N_D=3.74$; ~30% Al) than for the less Al rich site B2 ($N_D=4.57$; ~4% Al). However, the data for **5** $CeMn_{1.8}Al_{0.2}D_{\sim 3.5}$ (B1: $N_D=3.12$, ~3% Al; B2: $N_D=3.36$, ~12% Al) show the opposite trend, thus suggesting a more complex behaviour. Finally, an estimation of the maximum hydrogen site occupancies and hydrogen contents based on purely geometric grounds [12], i.e. without considering the influence of preferential occupancy of Al free metal tetrahedrons, yields values ($24l$: 1/2–1/3, $12k_2$: 1/3–2/3, $6h_2$: 0, $6h_1$: 1; $H_{max}=5.5$ H/f.u.) that differ significantly from those estimated previously for $CeMn_{1.5}Al_{0.5}D_{\sim 4.0}$ ($24l$: 1/4, $12k_2$: 1/2, $6h_2$: 0; $6h_1$: 1; $H_{max}=4.5$ H/f.u. [2]).

3.4. Magnetic properties

As shown in Fig. 3 the susceptibilities of the alloy **2** $CeMn_{1.8}Al_{0.2}$ and the deuteride **5** $CeMn_{1.8}Al_{0.2}D_{3.52}$ can be properly described with a modified Curie Weiss law $\chi=\chi_0+C/(T-\Theta)$ (χ_0 Pauli susceptibility, C Curie constant, Θ paramagnetic Curie temperature). The susceptibility of the alloy is dominated by an essentially temperature independent susceptibility χ_0 of $\sim 2.6(2)\cdot 10^{-3}$ emu/mol above 50 K. The low temperature upturn can be attributed to a Curie Weiss contribution of impurity phases (β-Mn and CeO_{1-x} see Section 2.1) corresponding to a rather low effective moment of about $\mu_{eff}=0.55(4)$ μ_B and to a paramagnetic Curie temperature of 16 K. The latter is indicative for ferromagnetic correlations, but no long range order occurs down to 2 K. For the deuterides **4** and **5** the analysis of the susceptibility data above 110 K yields a significantly smaller χ_0 of about $6(2)\cdot 10^{-4}$ emu/mol than for the parent compound but gives an effective moment of $\mu_{eff}=3.5(2)$ μ_B and 3.2(2) μ_B, respectively, which is close to that of trivalent Ce^{III} ($\mu_{eff}=3.6$ μ_B). The effective moment of the hydride **3** [3.2(2) μ_B] coincides with those of the deuterides. The remarkably large increase in effective moment by 3 μ_B under hydrogenation together with the big volume expansion provides strong evidence for a valence change $Ce^{IV}\rightarrow Ce^{III}$. The anomalous flattening of the susceptibility of the deuteride below 75 K together with the appearance of an irreversibility between field cooling (not shown for clarity) and zero field cooling is reminiscent to freezing of magnetic clusters over a rather broad range of temperatures. Freezing phenomena may arise from the fine granularity of the powder specimens. The transition at 75 K and the irreversibility exhibits a remarkable field dependence: The former is washed out and shifted to lower temperatures as external fields are increased and freezing diminishes at about 3 T. Although the fairly complex field and temperature dependence of the susceptibility for $T<80$ K does not allow a straightforward interpretation to be made, we suggest that the broad peak at 75 K in the zero-field cooling susceptibilities of the deuterides and the cusp at 70 K in the hydride arises from antiferromagnetic order within the grains of the fine powder.

4. Conclusion

$CeMn_{1.8}Al_{0.2}$, if carefully hydrided, absorbs more than 4.4 H atoms/f.u., thereby undergoing a very large volume expansion and a metal atom site exchange that is the first of that type reported in Laves phase structures. While the exchange as such is not surprising, the fact that it occurs over a distance of 2.7 Å at room temperature is remarkable. The exceptional mobility of the metal atom substructure during hydrogenation is enhanced by a valence transition of cerium and a structural segregation into manganese (aluminium) and binary cerium hydride. Both the volume expansion and the change from Pauli paramagnetism to local moment, i.e. Curie Weiss behaviour with an effective moment of 3.5 μ_B, provide evidence for a hydrogen induced valence transition $Ce^{IV}\rightarrow Ce^{III}$. The anomalous temperature and field dependence of the susceptibility of the deuterides and the hydride at low temperatures presumably arises from antiferromagnetic order within the grains at about 75 and 70 K, respectively, and seems to be complicated by freezing phenomena due to the fine granularity of the deuterided or hydrided powder.

Acknowledgements

The authors thank Y. Tokaychuk (Geneva) for help with the drawings and sample preparation for the magneto-

meter. This work was supported by the Swiss National Science Foundation and the Swiss Federal Office of Energy.

References

[1] T. Ohba, Y. Kitano, Y. Komura, Acta Crystallogr. C 40 (1984) 1–5.
[2] K.J. Gross, D. Chartouni, F. Fauth, J. Alloys Comp. 306 (2000) 203–218.
[3] P. Fischer, G. Frey, M. Koch, M. Könnecke, V. Pomjakushin, J. Schefer, R. Thut, N. Schlumpf, R. Bürge, U. Greuter, S. Bondt, E. Berruyer, Physica B 276–278 (2000) 146–147.
[4] R.H. Van Essen, K.H.J. Buschow, J. Less-Common Met. 70 (1980) 189–198.
[5] D. Fruchart, F. Vaillant, E. Roudaut, A. Nemoz, X.G. Tessema, Phys. Status Solidi A 65 (1981) K19–K24.
[6] D. Fruchart, F. Vaillant, A. Rouault, A. Benoit, J. Flouquet, J. Less-Common Met. 101 (1984) 285–290.
[7] J. Osterwalder, T. Riesterer, L. Schlapbach, F. Vaillant, D. Fruchart, Phys. Rev. B 31 (1985) 8311–8313.
[8] J.-L. Bobet, B. Chevalier, B. Darriet, M. Nakhl, F. Weill, J. Etourneau, J. Alloys Comp. 317–318 (2001) 67–70.
[9] P. Spatz, K. Gross, A. Züttel, F. Fauth, P. Fischer, L. Schlapbach, J. Alloys Comp. 261 (1997) 263–268.
[10] A.E. Dwight, in: Proceedings of the 7th Rare-Earth Research Conference, 1969, pp. 273–281.
[11] P. Spatz, K.J. Gross, A. Züttel, L. Schlapbach, J. Alloys Comp. 260 (1997) 211–216.
[12] D.P. Shoemaker, C.B. Shoemaker, J. Less-Common Metals 68 (1979) 43–58.